Interferometric Processing of Spaceborne SAR Data in Advanced SAR Imaging Modes

Josef Mittermayer and Alberto Moreira

Deutsches Zentrum für Luft- und Raumfahrt (DLR)
Institut für Hochfrequenztechnik und Radarsysteme
82234 Oberpfaffenhofen, Germany
T: +49-8153-28-2360, E-Mail: josef.mittermayer@dlr.de

Summary: The paper gives an analysis of ScanSAR and Spotlight data and identifies their common properties and the differences. A generic processing algorithm which consists of the Extended Chirp Scaling algorithm and the Frequency Scaling algorithm is proposed for high precision phase preserving processing of ScanSAR and SpotSAR imaging modes for future spaceborne SAR systems.

The ScanSAR processing perfomance is demonstarted by the inteferometric processing of Radarsat ScanSAR data. The SpotSAR processing is validated using raw data from the airborne experimental SAR-System (E-SAR) of DLR.

I. Introduction

ScanSAR and SpotSAR are two operation modes of SAR systems, which improve the standard stripmap mode of operation in two different ways.

In ScanSAR, the scene size in range is extended by scanning the antenna in elevation and alternating illumination of several subswaths. The raw data of one illumination of a subswath are denoted by raw data burst. Like in stripmap SAR, the scene extension in azimuth is principally only determined by the length of the overflight. By the scanning in elevation, the synthetic aperture length is reduced to the burst length. The full synthetic aperture, which corresponds to the azimuth beamwidth θ_a, is shared between the subapertures T_{si}. Due to the short burst length, the achievable azimuth resolution is reduced. Figure 1 shows the geometry in the ScanSAR mode of operation.

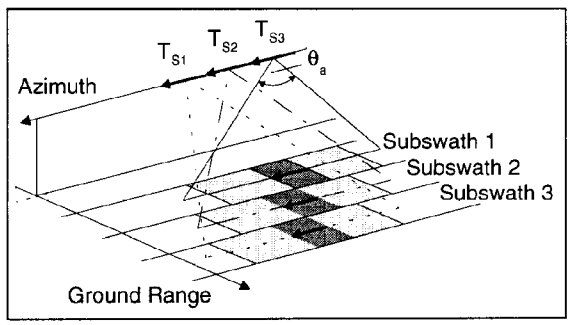

Figure 1: *ScanSAR geometry*

The basic difference between ScanSAR and conventional stripmap mode SAR is that each target is illuminated by different parts of the azimuth antenna pattern for a shorter time, the burst duration. This means each target has a different Doppler history depending on its azimuth position. ScanSAR shows a lot of interesting properties, which are for example discussed in [7].

In SpotSAR, the antenna is steered in azimuth direction in order to obtain an improved geometric resolution in azimuth. During the data acquisition, the antenna is constantly steered to scene center direction. This extends the illumination time and allows the generation of a long synthetic aperture, denoted by spotlight aperture in the following, which corresponds to a large Doppler bandwidth and thus, to a high azimuth resolution.

For a similar high range resolution, high bandwidth linear frequency modulated signals have to be transmitted. Due to the small range extension of a spotlight scene, the linear frequency modulation is usually removed before A/D-conversion in order to obtain a bandwidth reduction. This procedure is known as dechirp on receive (DOR) [2]. The DOR has two important impacts on the processing. First, it removes the linear frequency modulation, which for example prohibits a direct chirp scaling processing. Second, a quadratic phase term with range is introduced, which deteriorates the image quality if not compensated. This phase term is denoted by residual video phase (RVP) [1]. The RVP describes a range dependent time shift of the range signal.

As shown in Figure 2, the spotlight illumination in azimuth is fully described by the start and end squint angle, Ψ_{start} and Ψ_{end}, the scene center position and the azimuth beam angle θ_a. Instead of start and end squint angle, the start and end time of the illumination $t_{a,start}$ and $t_{a,end}$ can be used. The scene center defines the origin of the azimuth time and is located at the slant range position r_c.

The gray area in Figure 2 is the valid target area, which contains targets, constantly illuminated from $t_{a,start}$ to $t_{a,end}$. The bold lines show the limit of the azimuth illumination.

Paper presented at the RTO SET Symposium on "Space-Based Observation Technology", held on the Island of Samos, Greece, 16-18 October 2000, and published in RTO MP-61.

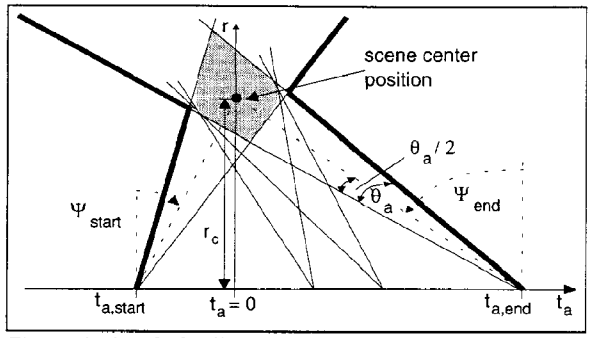

Figure 2: *Spotlight illumination geometry*

Due to the azimuth antenna steering in SpotSAR, the azimuth scene size is limited by the azimuth angle of the real aperture θ_a. The scene size in range is mainly determined by the antenna elevation pattern but also by the antenna steering. More information about the spotlight mode can be found for example in [4].

II. ScanSAR and SpotSAR Raw Data

The range modulation in SpotSAR and ScanSAR raw data is given by the modulation of the transmitted radar pulse, which is mostly a linear frequency modulation. In SpotSAR, often Dechirp on Receive is used before the A/D-conversion in order to transform the range signal into a superposition of sinusoidal signals with reduced bandwidth. In case of no Dechirp on Receive, the range modulation in SpotSAR and ScanSAR raw data is identical. Of course, the signal bandwidth in SpotSAR is normaly higher than in ScanSAR.

The azimuth modulation in SpotSAR raw data and in one ScanSAR raw data burst is inherently very similar since in both modes the azimuth illumination for all targets has the same start and end time. The high resolution Spotlight mode consists only of one raw data burst with a high number of range echo lines, while ScanSAR raw data consist of several hundreds of bursts with only several tens of range echo lines. In the following, one ScanSAR raw data burst and a complete set of SpotSAR raw data is considered.

The azimuth signals are different for different target azimuth positions, in contrary to Stripmap data. ScanSAR and SpotSAR azimuth signals show a different Doppler history, a different Doppler centroid and also a slightly variation of the azimuth bandwidth dependent on the azimuth position of a target. In stripmap data, the Doppler history and centroid as well as the azimuth bandwidth are independent of the azimuth position of a target.

On the other hand, the azimuth signal length in ScanSAR and SpotSAR is independent of the target range position while in Stripmap SAR the azimuth signal length is increasing with range. Due to constant length of the synthetic aperture with range, the ScanSAR and SpotSAR target azimuth bandwidth and resolution is strongly dependent on the targets range position. There is also a neglectable dependency on the target azimuth position. Stripmap mode data show an azimuth bandwidth and resolution independent on the range position. This is one of the well-known fundamentals of the standard stripmap SAR.

The following properties of the azimuth signals are identical in SpotSAR raw data and a single ScanSAR raw data burst:

- valid targets can be defined as targets with an azimuth illumination length equal to the full burst /spotlight aperture length
- the start and the end times of the azimuth illumination are equal for all valid targets independent of target range and azimuth position
- the azimuth signal is space-variant and depends on the azimuth position of the target
- the azimuth resolution is almost independent of the azimuth positioning of a target but shows noticeable dependency on the range position
- the azimuth processing can be performed by stripmap methods but this requires a large data overhead by zero padding, which makes the processing inefficient
- due to the constant illumination start and end times for all targets, SPECAN [9] is an efficient processing approach, which can be made highly accurate and phase preserving by azimuth scaling [4][7]

The target Doppler histories in a single ScanSAR raw data burst and in SpotSAR raw data are very similar, as is shown in Figure 3. The Doppler frequency is denoted by f_a, the azimuth time by t_a and the frequency histories are linearly approximated in the figure.

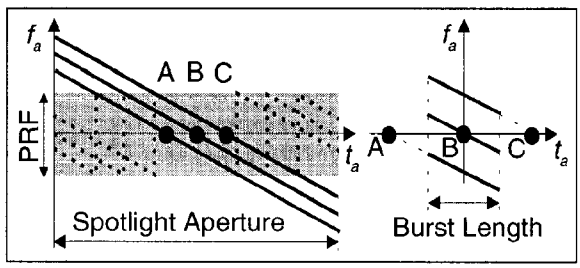

Figure 3: *Doppler history in SpotSAR (left) and ScanSAR (right)*

The left diagram shows the Doppler history of three targets A, B and C, located at different azimuth but identical range position for SpotSAR illumination. Spotlight raw data are acquired with a PRF sufficient for the instantainious bandwidth, which corresponds to the azimuth beam angle, but which is samaller than the total bandwidth of the Spotlight scene. The signals in the Spotlight raw data are ambiguous in azimuth frequency

and are shown in dashed style. The continuous lines show the unambiguous signals for a theoretically very high PRF.

The right diagram in Figure 3 shows the Doppler history of three targets at different azimuth but identical range position in a ScanSAR raw data burst. From the figure it is obvious that a similar azimuth processing can be applied to both, ScanSAR and SpotSAR due to the constant start and end times of the illumination, if the spotlight azimuth signal is made unambiguous, i.e. by subaperture processing [4].

III. The Generic ECS for ScanSAR and SpotSAR

A generic processing approach is presented, which is denoted by generic Extended Chirp Scaling (ECS) for ScanSAR and SpotSAR. It is composed of the Extended Chirp Scaling for ScanSAR and the Frequency Scaling Algorithm for SpotSAR.

A processing kernel is introduced, consisting of chirp scaling or frequency scaling for range processing and SPECAN, combined with azimuth scaling for the azimuth processing. This kernel is applied to both, ScanSAR and Spotlight raw data.

The range processing is performed by chirp scaling for ScanSAR and Spotlight SAR without Dechirp on Receive. For Spotlight data with Dechirp on Receive, the frequency scaling operation is used. Both methods require only multiplications and FFTs and use partially equal analytical expressions, although the derivation of chirp scaling and fequency scaling is different. The azimuth processing is also free of interpolations. The proposed generic processing method is thus very suitable for high accurate and efficient image and interferometric processing.

Different processing steps are added before and after the kernel for either ScanSAR or Spotlight processing. In ScanSAR, different single look complex (SLC) subswath images are generated for each possible azimuth look. From the SLC subswath pairs complete subswath interferograms are generated, which are later coherently added for a reduction of the phase noise. The number of possible azimuth looks is defined by the scanning strategy. In SpotSAR, a subaperture processing is applied, which reduces the requirements on the PRF during the processing to the PRF-value in the raw data and enables data blocks with short azimuth extension inside the algorithm kernel.

The block diagram of the generic formulation of the ECS for phase preserving SpotSAR and ScanSAR processing is shown in Figure 4. All parts in black letters on white background are used in ScanSAR and SpotSAR processing. Black letters on grey background mean usage only in SpotSAR processing and white letters mean usage only for ScanSAR.

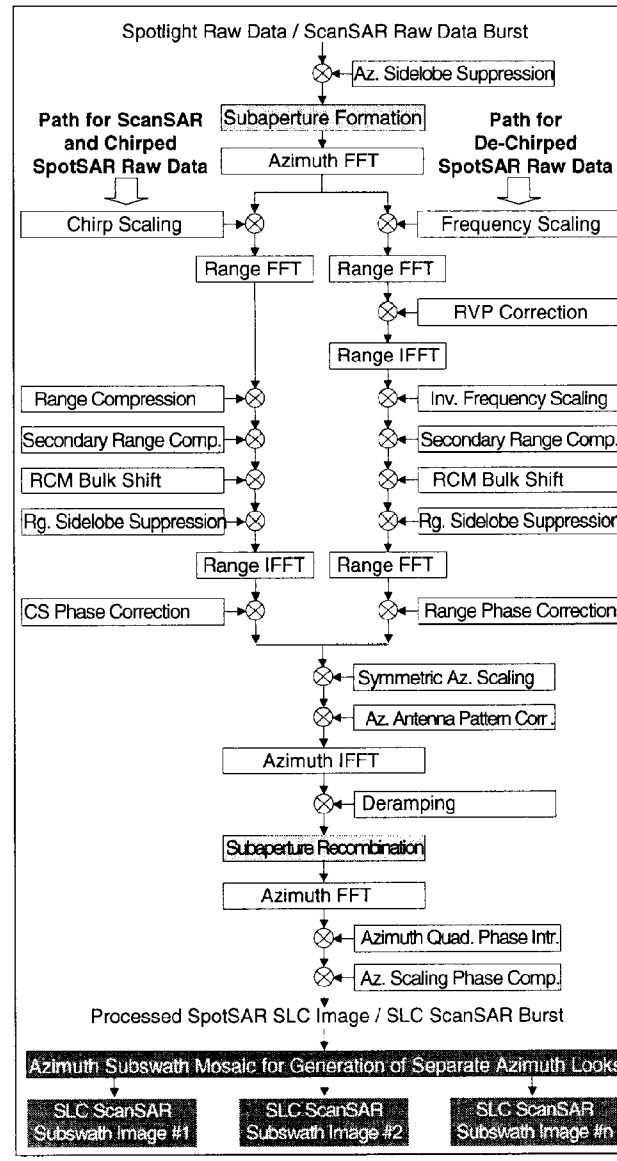

Figure 4: *Block diagram of generic ECS for SpotSAR and ScanSAR*

IV. Azimuth Processing

As shown in Figure 4, the azimuth processing starts with the weighting of the raw data for azimuth sidelobe suppression. This can easily be performed since in the raw data all azimuth signals are located at the same azimuth time position and the ECS is focussing in azimuth frequency domain. Next, the subaperture formation is performed in case of spotlight data for avoiding upsampling of the raw data in azimuth [4]. After transforming the data into range Doppler domain, either chirp scaling or frequency scaling is performed for full range compression and range cell migration correction, as will be explained in more detail in section V.

The azimuth processing is continued by azimuth scaling and the azimuth antenna pattern correction. The azimuth scaling transforms the azimuth modulation into a pure quadratic phase modulation which is independent of range [7] [4]. The possibility of selecting the final azimuth sampling distance during the azimuth scaling is very useful for exact co-registration of interferometric image pairs and for the mosaic of the single ScanSAR subswaths. The term symmetric azimuth scaling is due to an azimuth time shift during the azimuth scaling for a minimized symmetric azimuth time extension [4].

The azimuth pattern correction is important since the azimuth signal of a target is weighted by different parts of the azimuth antenna pattern dependent on the target azimuth position. If not corrected, an amplitude modulation is visible in the image. In ScanSAR, the pattern can be corrected accurately in azimuth frequency domain. For SpotSAR, the subaperture approach allows an approximated azimuth antenna pattern correction, which is the more accurate the smaller the subapertures are. The azimuth antenna pattern correction in SpotSAR can also be performed in the final image. The approximation there is the assumption that each target is always illuminated by the same portion of the antenna diagram.

After transforming the data into azimuth time domain, the deramping operation is performed by using a quadratic phase function, which is constant with range. In case of SpotSAR, the subapertures are recombined next. The azimuth compression is then performed by the final azimuth FFT, which is followed by a quadratic phase correction, required for phase preserving SPECAN processing and by an additional azimuth scaling phase correction, which is due to the azimuth time shift during the symmetric azimuth scaling.

After the phase corrections, the SpotSAR single look complex (SLC) image is available for further interferometric processing. In case of ScanSAR, the processed bursts have to be combined in order to form one SLC ScanSAR subswath image for each azimuth look. The number of possible azimuth looks is defined by the ScanSAR scanning strategy. From each interferometric SLC subswath image pair an interferogram can be generated and all these interferograms can be coherently added for phase noise reduction.

V. Range Processing

As can be seen in Figure 4, the range processing follows one of the two signal paths. The left signal path is for ScanSAR data and for SpotSAR data without Dechirp on Receive. The range processing in this path is performed analog to the range processing in the ECS algorithm [7] for stripmap. In case of spotlight with Dechirp on Receive, the right signal path has to be selected using the frequency scaling approach [4]. Both methods require only multiplications and FFTs and use partially equal analytical expressions. In case of chirp scaling, the weighting for range sidelobe suppression is performed in range frequency domain while the weighting in the frequency scaling approach is performed in range time domain.

VI. Interferometric Spotlight Processing of E-SAR Stripmpap Raw Data

The algorithm performance for SpotSAR is demonstrated using real raw data of the experimental SAR System (E-SAR) of DLR. However, the algorithm can easily be adopted to Spaceborne SpotSAR. The E-SAR is working in the stripmap mode but offers a wide beamwidth in azimuth and a high PRF. This allows the processing of relatively high resolution spotlight images. Figure 5 shows the principle of processing stripmap raw data in the spotlight mode.

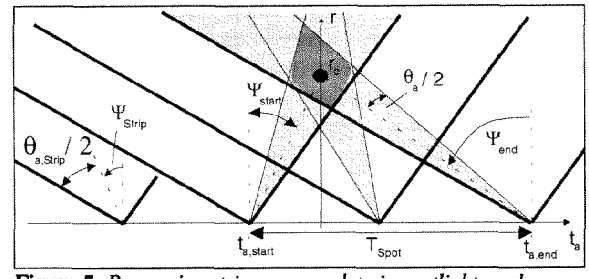

Figure 5: *Processing stripmap raw data in spotlight mode*

The thick lines in the figure show a stripmap illumination with fixed squint angle Ψ_{strip} and a beamwidth $\theta_{a,strip}$. For the spotlight image, the bright gray sectors have to be selected, which correspond to the spotlight beamwidth θ_a. This results in a different squint angle for each azimuth position within the interval $[\Psi_{start}; \Psi_{end}]$.

As a reference, the detected image of a stripmap processed E-SAR raw data set is shown in Figure 6. The azimuth beamwidth is 8° and the instantaneous bandwidth is 780 Hz, from which 270 Hz were processed to 0.42 m azimuth resolution. The range resolution is 2.16 m. The scene size is about 480 m in azimuth (horizontal) by 530 m in range. The spotlight image processed from the same raw data is shown in Figure 7. The spotlight beamwidth is set to 5.3° and the resulting squint angle variation is 2.8°. This means an azimuth bandwidth of 283 Hz in near and 257 Hz in far range, corresponding to azimuth resolutions of 0.40 and 0.44 m. The range resolution is as in the stripmap image.

A more conspicuous difference between the stripmap and the spotlight image is marked by the white circles. The edge of a building is more visible is the spotlight image. For the squint angle of the stripmap illumination, the reflection was less than for the squint angle of the spotlight illumination at this position in the image. Figure 8 shows the stripmap spotlight difference image. In the middle of the image, there is no difference visible since the focussing in stripmap and spotlight mode was over the same squint angle range. To the left and right side, the differences are

growing, due to the different squint angle ranges. Also the coherence map in Figure 9 shows the conformity in the middle of the images and the increasing non-conformity to the left and right side. High coherence is encoded towards white while low coherence is encoded towards black.

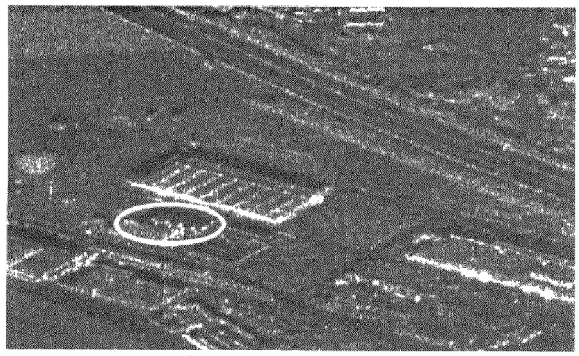

Figure 6: *Detected stripmap image*

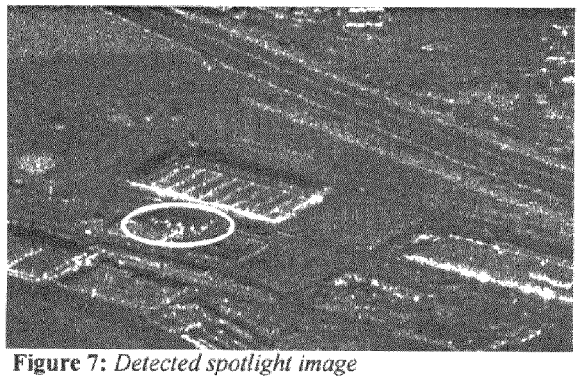

Figure 7: *Detected spotlight image*

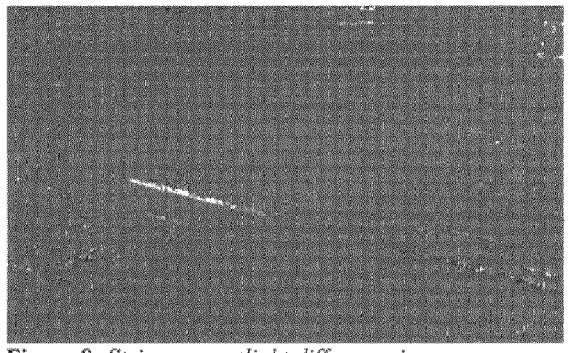

Figure 8: *Stripmap spotlight difference image*

The result of the interferometric Spotlight processing is shown in Figure 11 while Figure 10 shows the stripmap interferogram of the same scene as a reference. The stripmap spotlight difference interferogram is shown in Figure 12. The height information in the stripmap and spotlight interferogram is principally identical. Small differences exist for targets, which are only visible from a certain observation angle. Other differences arise in shaded areas, where only noise is processed from different squint angle ranges. Both interferograms are identical in the center of the image, since the center is focussed over the same squint angle range and shows the same phase noise. To the left and right side, the difference in the phase noise is increasing since different spectral components are processed.

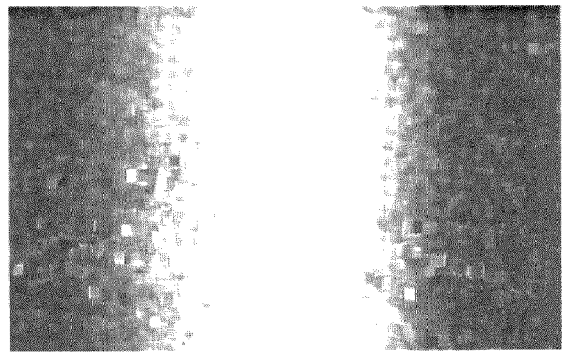

Figure 9: *Coherence map of stripmap and spotlight channel 1*

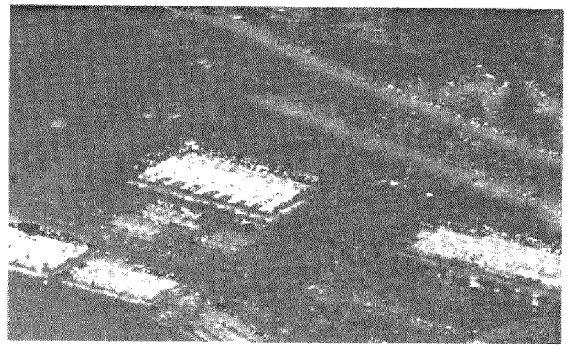

Figure 10: *Stripmap interferogram*

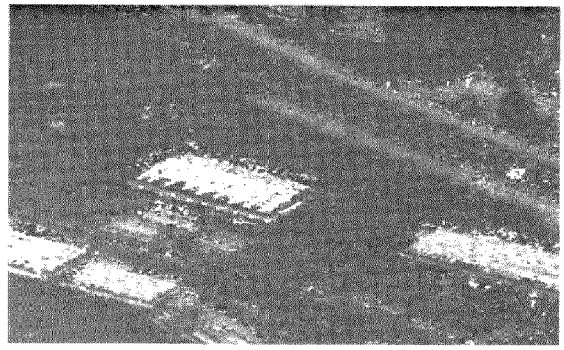

Figure 11: *Spotlight interferogram*

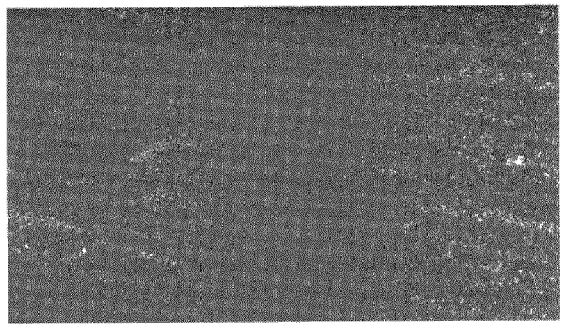

Figure 12: *Stripmap spotlight difference interferogram*

VII. Interferometric ScanSAR Processing

With courtesy from CSA, Radarsat ScanSAR data within the CCRS ADRO Proposal #500 were used for the processing. The same data had also been processed using an azimuth time domain convolution approach combined with DLR's BSAR processor [1].

After the subswath processing following the generic ECS of Figure 4, an image domain range multilooking was applied to one detected SLC subswath image and to the amplitude azimuth multilook image by a moving average with a window length corresponding to 3 range looks. The image detected from one SLC subswath is shown in Figure 13. Interesting image parameters are listed in Table 1.

number of processed bursts	137
corresponding scene extension azimuth	181 km
subswath W1 extension in slant range (196 km extension in ground range)	78 km
number of selected range echo lines within a burst	64
corresponding azimuth resolution	68m (near) 74m (far)
number of range looks	3
resolution slant range	11.6 m

Table 1: *Subswath processing parameters*

The image of a part of the Barthust Island in Canada shows land surface, ocean and ice areas. Compared to Figure 14, which shows the multilook image with 3 range and the two azimuth looks, more speckle is obvious in the single azimuth look image. The scalloping is much higher in the azimuth single look image but due to the lower speckle, the scalloping can be better observed in the azimuth multilook image.

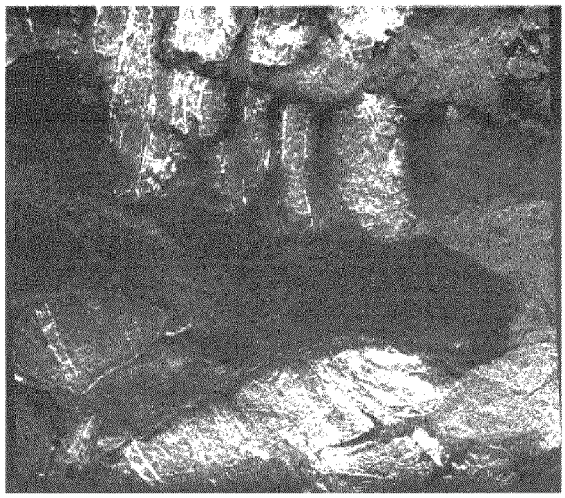

Figure 13: *Image detected from one azimuth look*

This can be seen in Figure 15, which shows the azimuth amplitude profiles of a part of the single azimuth look image at the bottom and the corresponding profile of the azimuth multilook image at the top.

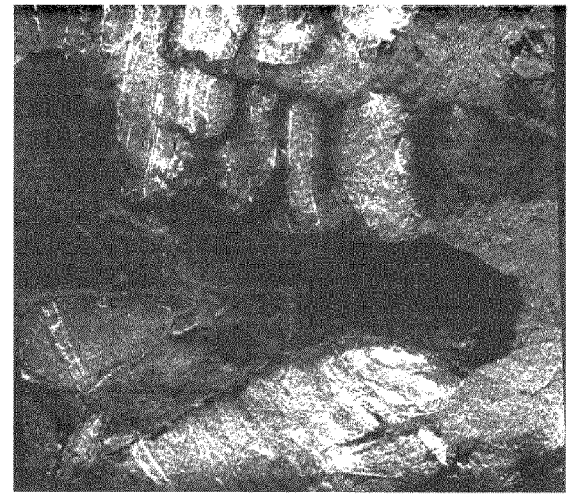

Figure 14: *Detected image with azimuth multilook*

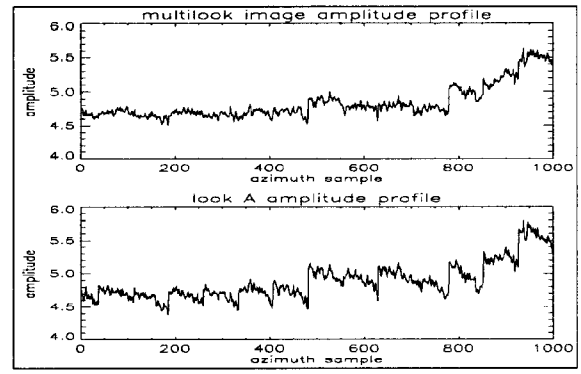

Figure 15: *Scalloping shown by azimuth profiles*

The interferometric processing starts already before the subswath processing by the selection of the raw data echo lines, which contribute to the same area on the ground [1]. For the processed Radarsat data set, this reduces the number of valid echo lines within a burst from 112 down to 64, corresponding to the azimuth resolution of about 70 m.

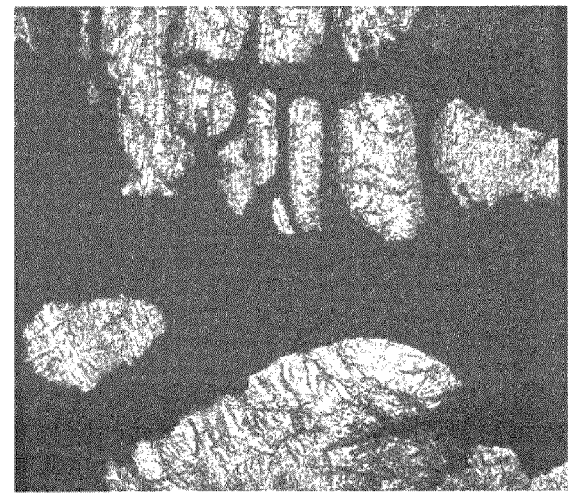

Figure 16: *Coherence map of azimuth look 1*

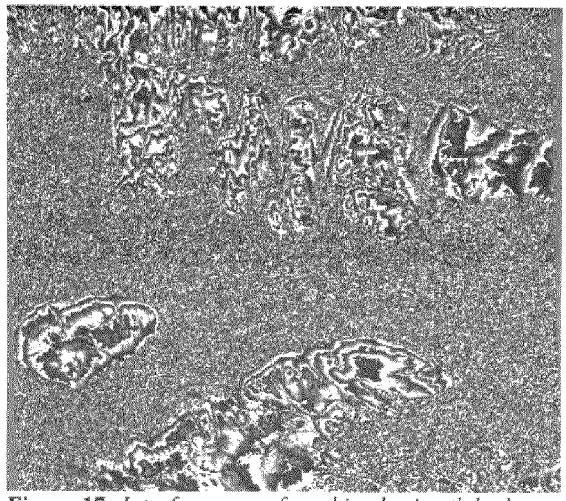

Figure 17: *Interferogram of combined azimuth looks*

A Range scaling [6] as well as the wavenumber shift [3] are applied during the subswath processing. We estimated a difference in the distance from near to far range of about 30 m between master and slave, which corresponds to 2.6 range samples. The introduced wavenumber shift was 2 MHz, while the transmitted bandwidth was 11.7 MHz.

After subswath processing, the interferometric multiplication of the master SLC subswath images with the conjugated slave SLC subswath images was carried out separately for each azimuth look. Then, after flat earth subtraction, a phase noise reduction was performed by a complex moving average in range on the two single azimuth look interferograms.

Figure 16 shows the coherency map of one azimuth look interferogram. The two data sets have been acquired with a time separation of 25 days and thus, almost only the land surface contributes to the interferogram. From the coherency histogram in Figure 18, a mean coherency of about 0.75 can be estimated for the land surface. The peak at 0.25 is due to the large ice areas with high temporal decorrelation.

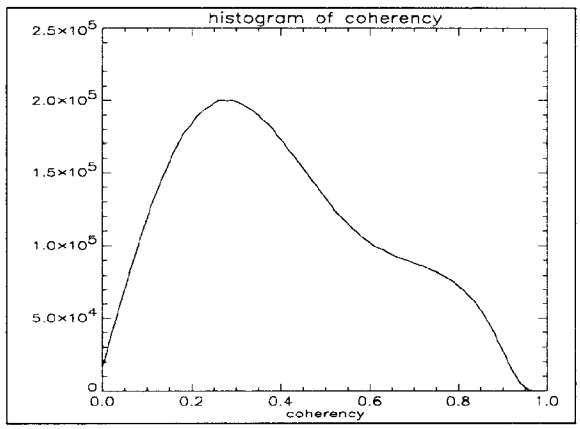

Figure 18: *Histogram of coherency for look A*
The multilook interferogram resulting from the coherent addition of the two SLCS interferograms is shown in Figure 17 after flat earth subtraction and a phase reduction by a moving average in range. The difference in the phase noise between azimuth single and multilook interferogram can't clearly be seen with the scale of Figure 17.

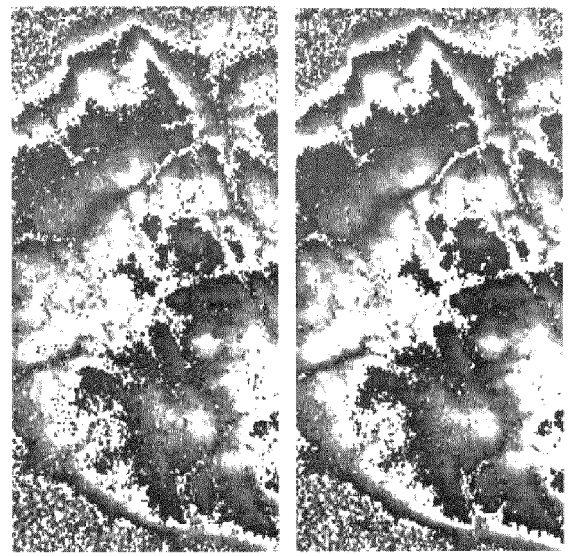

Figure 19: *Single look (left) and multilook (right) interferogram*

The small parts of the interferograms in Figure 19 allow a better observation of the difference in the phase noise. The single azimuth look interferogram is on the left and the multilook interferogram is on the right.

VIII. Conclusions

This paper shows the similarities between ScanSAR and SpotSAR and demonstrates how these similarities can be exploited by using a generic formulation of the ECS for the processing. The generic formulation provides advantages for the processor implementation in hard- or software and off-line or real-time since equal or very similar processor modules can be used for both, ScanSAR and SpotSAR data processing.

The good performance in interferometric ScanSAR and SpotSAR processing was shown by processing an interferogram from Radarsat ScanSAR data and from the generation of a SpotSAR interferogram from E-SAR data.

IX. References

[1] R. Bamler et al.: "RADARSAT SAR Interferometry Using Standard, Fine and ScanSAR Modes", Proc. of Radarsat ADRO Final Symposium, Montreal-Canada, 1998.

[2] G. Carrara, R. S. Goodman, R. M. Majewski: "Spotlight Synthetic Aperture Radar", Artech House Boston, London, 1995.

[3] F. Gatelli et al.:"The Wavenumber Shift in SAR Interferometry", IEEE Transactions on Geosc., Vol. 32, No. 4, July 1994, pp. 855-865.

[4] J. Mittermayer, A. Moreira, O. Lofeld: "Spotlight SAR Data Processing Using the Frequency Scaling Algorithm", IEEE Trans. on Geosc. and Remote Sensing, Vol. 37, No. 5, September 1999.

[5] Mittermayer, J., A. Moreira and O. Loffeld: "Comparison of Stripmap and Spotlight Interferometric SAR Processing using E-SAR Raw Data". Proc. of EUSAR 2000.

[6] Mittermayer, J., A. Moreira: "The Extended Chirp Scaling Algorithm for ScanSAR Interferometry". Proc. of EUSAR 2000.

[7] A. Moreira, J. Mittermayer and R. Scheiber, " Extended Chirp Scaling Algorithm for Air- and Spaceborne SAR Data Processing in Stripmap and ScanSAR Imaging Modes", IEEE Trans. on Geosci. and Remote Sensing, Vol. 34, NO. 5, September 1996.

[8] R. K. Raney, Runge, H., Bamler, R. Cumming, I. and Wong, F.: "Precision SAR Processing without Interpolation for Range Cell Migration Correction". IEEE Trans. on Geosci. and Remote Sensing, Vol.32, No.4, July 1994.

[9] Sack, M., Ito, M.R., Cumming, I.G.: "Application of Efficient Linear FM Matched Filtering Algorithms to SAR Processing". IEE Proc.-F, Vol.132, No.1, 1985. pp. 45-57.